Hearing Research 481 (2026) 109781

Contents lists available at ScienceDirect

Hearing Research

journal homepage: www.elsevier.com/locate/heares

Research paper

Close-to-critical Hopf oscillators boost cochlear gain in realistic models with fluid focusing

Renata Sisto [a], Arturo Moleti [b],*

[a] INAIL, DIMEILA, Monte Porzio Catone (RM), 00074, Italy

[b] Department of Physics, University of Rome Tor Vergata, 00133 Rome, Italy

ARTICLE INFO

Keywords:
Cochlear mechanics
Nonlinear dynamics
Hopf oscillators
Critical behavior

ABSTRACT

Critical Hopf oscillators have been proposed for modeling the cochlear micromechanics, and the generation of spontaneous otoacoustic emissions. In such top-down models, the cochlear micromechanical elements are abstractly represented through equations written in normal form. There is a gap to be filled between this abstract formulation and the complexity of the motion of the Organ of Corti as revealed by recent optical coherent tomography measurements. The aim of the present work is bridging this gap using a bottom-up approach: starting from realistic equations schematizing the actual physical elements of cochlear micromechanics, we show explicitly how these equations admit a normal form representation. To do that, the Organ of Corti is schematized as a system of two oscillators coupled by an internal active low-passed nonlinear force, and to an incompressible 2D fluid. We generalize the classical two-equation normal form to a three-equation system, demonstrating that the normal form approach may be used to compute the relative motion of the main elements of the Organ of Corti, while the center of mass motion depends on the fluid forces only. This way, the parameters of the critical oscillator are no longer abstract mathematical quantities, but acquire a direct physical interpretation in terms of the dynamics of the underlying physical elements. In particular, the approach to the critical behavior, and the consequent dramatic variation of the cochlear response gain and bandwidth, are quantified in terms of a few dimensionless parameters of obvious physiological meaning.

Nonlinear oscillators working near a Hopf bifurcation exhibit exceptional properties in terms of gain and tuning that have suggested using them to model the resonant elements of the hearing system, from both the perceptual (Cartwright et al., 1999) and the mechanical (Jülicher et al., 2009) viewpoint. A classical study (Eguíluz et al., 2000) summarizes the main properties of the response of a Hopf oscillator: occurrence of self-sustained oscillations, essential cubic nonlinearity (down to very low stimulus levels) and an inverse proportionality relation between the response nonlinearity and the bandwidth nonlinearity. Although such a relation is not observed in the real cochlea, close-to-critical behavior has been invoked to justify the high gain and tuning of mammalian hearing.

It is well-known that single oscillator models cannot fully represent the response of the Organ of Corti (OoC), yet critical behavior may occur also in mechanically complex models. Berger and Rubinstein (2021) proposed a modular model for a slice of the OoC, which applies Newton's law to the interaction among all its mechanical and fluid elements, including the role of the subtectorial fluid. Their model shows that critical behavior may be predicted for the internal behavior of the OoC, which may be interpreted as the existence of a second filter between the BM motion and the IHC vibration, improving both frequency selectivity and gain. Lee et al. (2016) provided experimental evidence for a similar role being played in the real cochlea by the strong radial tuning of the RL and TM, at a frequency lower than the local BF of the BM motion. Recently, ver Hulst (2024) demonstrated that Hopf oscillators can be successfully used for modeling also the tall and broad basilar membrane response if the 2D hydrodynamics is also included, solving the discrepancy with the observed decoupling between gain and tuning (Sisto et al., 2015). Cochlear models should also be able to predict other observable quantities, namely the observed relation between the RL and BM motion (Cooper et al., 2018; Cho and Puria, 2022), and to explain the relatively flat and level-independent BM admittance function that has been inferred from pressure measurements near the BM (Dong and Olson, 2013).

This study will focus on two-degrees-of-freedom (2DOF) 2D transmission-line cochlear models (Neely and Kim, 1986; Sisto et al., 2021). Such models can be considered as a first step in our attempt to connect the single-oscillator cochlear modeling approach to more anatomically accurate descriptions of the cochlear function. In this

* Corresponding author.
E-mail address: moleti@roma2.infn.it (A. Moleti).

https://doi.org/10.1016/j.heares.2026.109781
Received 10 July 2026; Received in revised form 19 August 2026; Accepted 19 August 2026
Available online 28 August 2026

schematization, each element of the OoC consists of two mechanical oscillators (hence 2DOF), e.g., the basilar membrane (BM) and the reticular lamina (RL), coupled by the internal active force associated with the outer hair cells (OHCs). The fluid fields (pressure and velocity) are coupled to the BM motion by incompressibility and viscous forces, and a 2D or 3D representation of the fluid is necessary to capture some of the major features of the cochlear phenomenology (Sisto et al., 2023). In this study we will show how the relative motion of the system may be formally represented by the normal form of a first order differential equation in a complex variable z describing a nonlinear oscillator close to a Hopf bifurcation. The normal form of this equation includes both the dynamics of the relative motion of two mechanical elements of the Organ of Corti (OoC), and the low-pass behavior of the active force generator associated with the outer hair cells (OHCs), exploiting the rather obvious fact that the motion of the center of mass depends only on the linear equation driven by the external forces (fluid differential pressure and viscous drag) applied to the Organ of Corti. Such an equivalence is shown starting from the description of the 2DOF model by Sisto et al. (2019, 2021), Sisto and Moleti (2021) and Sisto et al. (2023), which was originally developed without any reference to critical oscillators. One of the main purposes of this study is to show that Hopf oscillators are not just abstract representations with fascinating dynamical properties, but that a sufficiently realistic cochlear model describing the main features of the cochlear response may admit such a representation of its local elements. Having done that, one can appreciate how well-known features of the critical oscillators may be reinterpreted in terms of optimal values of the physical parameters of the real system. We will also show that an extension of the original model to three equations is necessary to recover the expected connection between high gain, sharp tuning, and approach to the critical regime.

1. Models

A didactic approach will be followed (for a more comprehensive introduction, see e.g., Moleti and Sisto (2025)), providing a basic formal introduction to both the normal form of critical oscillator equations and the recent developments of 2D, 3D transmission-line cochlear models including fluid focusing and viscous damping. This approach is motivated by the necessity of developing a bridge of common theoretical knowledge joining two rather separated communities of researchers. We will start considering a one-degree-of-freedom (1DOF) model, in which each element of the OoC at a given longitudinal position x is represented by the basilar membrane (BM) only, of mass per unit surface $M(x)$, driven by the differential pressure. The equation of motion is:

$$M(x)\ddot{\xi}(x,t) + C(x)\dot{\xi}(x,t) + K(x)\xi(x,t) = -p_d(x,t). \tag{1}$$

Here, and in the following, dots indicate, for brevity, the time partial derivatives, as the differential pressure $p_d(x,t)$ and the local BM displacement $\xi(x,t)$ are functions of the longitudinal cochlear position x and time t. $C(x)$ and $K(x)$, representing the BM viscous coefficient and stiffness per unit surface, are both scaling functions of x. The model may be extended to include nonlinear instantaneous active terms modeling the OHC additional force. Recalling the 1D propagation equation for the pressure along x:

$$\frac{\partial^2 p_d(x,t)}{\partial x^2} = -2\frac{\rho}{H}\ddot{\xi}(x,t), \tag{2}$$

where ρ is the fluid (perilymph) density and H is the height of each scala (tympanic and vestibular), which in more realistic models, is a function of x, to account for cochlear tapering (Altoè and Shera, 2020). In the linear limit, one can use the frequency domain formulation (here and in the following, we use, for each Fourier Transform, the same name as that of the corresponding time-domain function). Using the definition of admittance as the complex ratio between BM velocity and pressure:

$$\ddot{\xi}(x,\omega) = i\omega\dot{\xi}(x,\omega) = i\omega Y_{bm}(x,\omega)p_d(x,\omega), \tag{3}$$

Eqs. (1), (2) can be written in the frequency domain as:

$$\frac{\partial^2 p_d(x,\omega)}{\partial x^2} = -k^2(x,\omega)p_d(x,\omega), \tag{4}$$

with:

$$k^2(x,\omega) = -2i\omega\frac{\rho}{H}Y_{bm}(x,\omega). \tag{5}$$

Note that in the 1D, or long-wave, approximation, the admittance is proportional to the wavenumber squared. We use the Wentzel–Kramers–Brillouin (WKB) approximation to find a traveling wave solution for the differential pressure field as a function of x and ω. Then, the BM velocity $\xi(x,\omega)$ is obtained using the admittance function, as:

$$\xi(x,\omega) = Y_{bm}(x,\omega)p_d(x,\omega). \tag{6}$$

From now on, we will omit, for brevity, the explicit dependence on time, frequency and position of all the functions and their FTs, as it should be implicitly obvious in each specific context.

1.1. From 1DOF to 2DOF

Recent 2DOF transmission-line models of the Organ of Corti (OoC) (Sisto et al., 2019, 2021, 2023), based on the original model by Neely and Kim (1986), assume an internal force between two oscillators (labeled 1 and 2, representing, respectively, the BM and the RL), associated with the outer hair cell (OHC) active elements, while the external force associated with the differential fluid pressure, applied to the BM only, accelerates the center of mass of the system. The equations describing the system in the time domain are:

$$\begin{aligned}
&M_1\ddot{\xi}_1 + C_1\dot{\xi}_1 + K_1\xi_1 \\
&= -C_3(\dot{\xi}_1 - \dot{\xi}_2) - K_3(\xi_1 - \xi_2) + C_{nl}(\dot{\xi}_1 - \dot{\xi}_2) - p_d, \\
&M_2\ddot{\xi}_2 + C_2\dot{\xi}_2 + K_2\xi_2 \\
&= C_3(\dot{\xi}_1 - \dot{\xi}_2) + K_3(\xi_1 - \xi_2) - C_{nl}(\dot{\xi}_1 - \dot{\xi}_2)), \\
&\frac{\partial^2 p_d}{\partial x^2} = -2\frac{\rho}{H}\ddot{\xi}_1.
\end{aligned} \tag{7}$$

where the dependence on x of the mass, damping, and stiffness functions is not explicitly stated, for brevity. The internal OHC force is modeled here as a phenomenological explicit antidamping term. In the linear limit, the coefficient C_{nl} is a constant, while in general it would be a nonlinearly decreasing function of the instantaneous local displacement and/or velocity. As for the 1DOF case, in the linear limit, we can rewrite the system in the frequency domain: if we call Z_1, Z_2, and Z_a the impedance functions associated, respectively, with oscillator 1 and 2 and to the internal coupling between them, the BM admittance function can be written as:

$$Y_{bm} = \frac{Z_2 + Z_a}{Z_a(Z_1 + Z_2) + Z_1 Z_2}, \tag{8}$$

where:

$$\begin{aligned}
Z_1 &= i\omega M_1 + C_1 - \frac{iK_1}{\omega} \\
Z_2 &= i\omega M_2 + C_2 - \frac{iK_2}{\omega} \\
Z_a &= C_3 - C_{nl} - \frac{iK_3}{\omega}.
\end{aligned} \tag{9}$$

1.2. Introducing low-pass filtering of the OHC force

In Sisto and Moleti (2021), a third dynamical equation is added to the 2DOF nonlinear model (Sisto et al., 2019), to represent the low-pass filtering effect due to the slow build-up of the OHC transmembrane potential, whose characteristic cutoff time is determined by the local conductance and capacitance of the OHC membrane. As suggested by physiologically based models of the OHC mechanism (Lu et al., 2006; Iwasa and Adachi, 1997), the force is represented here by a low-passed elastic term, which substitutes the antidamping term of Eq. (7), with a similar effect. The model equations in the time domain become:

$$\begin{aligned}
&M_1\ddot{\xi}_1 + C_1\dot{\xi}_1 + K_1\xi_1 \\
&= -p_d - C_3(\dot{\xi}_1 - \dot{\xi}_2) - K_3(\xi_1 - \xi_2) + p_{OHC} \\
&M_2\ddot{\xi}_2 + C_2\dot{\xi}_2 + K_2\xi_2 \\
&= C_3(\dot{\xi}_1 - \dot{\xi}_2) + K_3(\xi_1 - \xi_2) - p_{OHC} \\
&\dot{p}_{OHC} + \frac{p_{OHC}}{\tau} = -\frac{K_{nl}}{\tau}(\xi_1 - \xi_2) \\
&\frac{\partial^2 p_d}{\partial x^2} = -2\frac{\rho}{H}\ddot{\xi}_1. \qquad (10)
\end{aligned}$$

The elastic coefficient K_{nl} describes a linear approximation to the actually nonlinear OHC internal force. This approximation may roughly describe the cochlear response at a given stimulus level, by assuming a global variation of K_{nl}, decreasing with stimulus level. In a nonlinear model, $K_{nl}(\dot{\xi}, \xi)$ would be a compressive nonlinear function of the local instantaneous displacement and/or velocity. Low-pass filtering implies two competing effects: as frequency gradually increases above the local cutoff frequency:

- attenuation of the response gradually decreases the effectiveness of the OHC force in the high-frequency range, above the local cutoff frequency. This negative effect has been often overemphasized, as discussed by Altoè and Shera (2023).
- rotation of the phase gradually increases the anti-damping nature of the OHC force, which would be approximately elastic below the cutoff frequency, so it may effectively transfer power to the mechanical system (Sisto and Moleti, 2021).

1.3. From 1D to 2D

A crucial step towards a realistic representation of cochlear hydrodynamics is overcoming the incorrect 1D assumption that the fluid variables are functions of the longitudinal coordinate only (and that the fluid velocity has only a longitudinal component). This step is accomplished in 2D models by introducing the dependence on the vertical coordinate z. Neglecting the viscous terms in the Navier–Stokes equations one can get the 2D propagation equation for the differential pressure in the time domain:

$$\int_0^H \frac{\partial^2 p_d}{\partial x^2} dz = -\rho\ddot{\xi}. \qquad (11)$$

This equation relates the BM transverse acceleration to the integral of the second spatial derivative of the pressure with respect to x, yielding the slow TW. The relation between the pressure at $z = 0$ and the pressure averaged along the z direction can be calculated in the frequency domain, taking into account (Steele and Taber, 1979; Duifhuis, 2012) the exponential dependence on z of the pressure field, computed in the 2D WKB approximation:

$$p_d(x, z, \omega) = \frac{f(x,\omega)\cosh(\kappa(H - z))}{\cos(\kappa H)} e^{-i\int_0^x \kappa(\omega,x')dx'}, \qquad (12)$$

and the fluid incompressibility, where f is a normalization function (Duifhuis, 2012). Here we use the greek letter κ for the wavenumber, to avoid confusion with the elastic constant. Integrating the exponential profile of the pressure over the vertical direction, the following relation can be obtained between the average pressure and the local pressure close to the BM:

$$\bar{p}_d = \frac{p_d(z = 0)}{\alpha(\kappa)}, \qquad (13)$$

where the function $\alpha(\kappa)$ is given by:

$$\alpha(\kappa) = \frac{\kappa H}{\tanh(\kappa H)}. \qquad (14)$$

The function α tends to unity in the long-wave region (for $\kappa H \ll 1$, the pressure is almost constant along the vertical axis) whilst it tends to κH in the short-wave region (for $\kappa H > 1$). It contributes to the cochlear gain, giving a boost to the differential pressure driving the BM in the short-wave region. The propagation equation for the average differential pressure can be written as:

$$\begin{aligned}
\frac{\partial^2 \bar{p}_d}{\partial x^2} &= -2\frac{\rho}{H}\ddot{\xi} = -\frac{2i\omega\rho}{H} Y_{bm} p_d(z = 0) \\
&= -\frac{2i\omega\rho}{H} Y_{bm}\alpha\bar{p}_d = -\kappa^2\bar{p}_d. \qquad (15)
\end{aligned}$$

The WKB solution for $\bar{p}_d$ may be used, along with Eq. (14), to get a solution for $p_d(z = 0)$, and ξ as a functions of ω and x. We can easily see that, while in the long-wave limit ($\alpha = 1$) the wavenumber squared is proportional to the admittance, in the short-wave limit, in which $\alpha = \kappa H$, the wavenumber is directly proportional to the admittance:

$$\kappa \approx -2i\rho\omega Y_{bm}. \qquad (16)$$

As the admittance is a given function of x, whose real part increases approximately as $\omega^2(x)$ in the region basal to the peak, a wavenumber proportional to the admittance grows much faster with x than in the long-wave case. The general relation between the wave vector and the admittance is nonlinear:

$$\kappa^2 = -2i\frac{\rho\omega\alpha(\kappa)}{H} Y_{bm}. \qquad (17)$$

We have discussed so far the solution of 1D transmission-line cochlear models with different numbers of degrees of freedom at each place x, in which the fluid effect was inserted in the WKB frequency-domain solution through the α function (Duifhuis, 2012; Shera et al., 2005; Sisto et al., 2021). The same effect can be kept into account in the 2D time-domain solution of transmission line cochlear models using the Green functions calculated in the late 1970's by Allen (1977) and Allen and Sondhi (1979), with the possibility of introducing explicitly, if assumed by the model, instantaneous nonlinearity of the OHC mechanism. In this study, we will not follow this approach, and focus on the properties of the linearized system, whose physical interpretation is relatively simpler.

1.4. Introducing viscous damping

The next step towards a realistic cochlear model is introducing the effect of fluid viscous damping on the vibrating elements of the OoC. In the short-wave region, the sharp velocity gradients associated with the large value of the wavenumber imply strong viscous dissipation, thus the ideal (non-viscous) fluid approximation must be abandoned. Including fluid viscosity in the model, a damping term appears in the admittance, associated with the interaction between the moving elements of the OoC and the fluid. Like focusing, this term is an increasing function of the wavenumber. Additional damping terms could be introduced in more accurate models of the OoC, associated with the internal viscoelasticity of the cells. To solve Eqs. (17) and (14), self-consistency of the system of equations is imposed using an iterative procedure (Sisto et al., 2021).

The total friction force in the z direction acting on both faces of the BM ($z = 0$) can be calculated as the vertical projection of the strain tensor:

$$\mu(\vec{\nabla}\vec{u} + (\vec{\nabla}\vec{u})^T) \qquad (18)$$

$$F_{frict}(x, t) = -4\mu \frac{\partial w(x, z, t)}{\partial z}\bigg|_{z=0}. \qquad (19)$$

In which w is the z component of the fluid velocity. Due to the adhesion boundary condition, the vertical fluid velocity in the boundary layer is coincident with the BM vertical velocity:

$$\dot{\xi} = w(z = 0) \qquad (20)$$

Therefore, this damping term can be written in the frequency domain as:

$$F_{frict} = -4i\omega\mu\kappa\xi, \tag{21}$$

where ξ is a function of position and frequency representing the instantaneous BM displacement. In a more refined model, the analog friction force applied to the RL could also be taken into account, as well as the contribution to the TW of the RL motion (Sisto and Moleti, 2025). Here they are both neglected for simplicity, due to the smaller local velocity (and velocity gradient) field at the top of the OoC. This viscous force, which, as the focusing effect, is proportional to the wavenumber, counteracts it, providing stability to the system also in the linear approximation (Sisto et al., 2021). This feature avoids the sharp saturation of the response to the nonlinear saturation "threshold" that is typical of unstable systems stabilized by the compressive nonlinearity associated with the decrease of the effectiveness of the OHC activity with increasing OoC velocity/displacement. The anti-damping OHC force provides the power input necessary to compensate the viscous losses of the forward TW in the peak region (Sisto et al., 2023; Sisto and Moleti, 2024).

A relevant feature of this picture is that the TW peak occurs well before reaching the "resonant" place. As also suggested by experiments (Dong and Olson, 2013), the sharp peak of the BM and RL response is not associated, as in a normal resonance, with a sharp maximum of the admittance, where the real part of κ vanishes (where $f/CF = 1$), but it occurs basally to that place. The broadband nature of the admittance function is explained by the compensation between the OHC effective antidamping term and the viscous damping terms within a broad region, in which the wavenumber remains almost completely real. With increasing stimulus level, the decreased effectiveness of the OHC mechanism implies a basal shift of the peak, where the maximum value of the wavenumber that the OHC mechanism can sustain against viscous losses is reached (Sisto et al., 2023; Sisto and Moleti, 2024). Introducing viscous damping in the linearized version of the problem means correcting the admittance function including a damping term proportional to the wavenumber, which requires using a recursive self-consistent procedure (Sisto et al., 2023).

1.5. Critical oscillators and the Hopf bifurcation

Nonlinear oscillators working at (or near) the Hopf bifurcation have been used to model the hair bundle (Jülicher et al., 2009), to explain the existence of spontaneous otoacoustic emissions (SOAEs) and the BM response nonlinearity (Duifhuis, 2012; ver Hulst, 2024).

Hopf oscillators work close to an instability controlled by compressive nonlinearity. Compressive nonlinear response is predicted at all stimulus levels, with gain decreasing with stimulus pressure S as $S^{-2/3}$. Unfortunately, for an isolated oscillator of this kind, a bandwidth increasing as $S^{2/3}$ is also predicted, which is not in agreement with experiments. Indeed, experiments on laboratory animals consistently show a "tall and broad" BM response, with a bandwidth weakly dependent on the stimulus level. It has recently been shown (ver Hulst, 2024) that such oscillators, used as tonotopic elements of a transmission-line cochlear model, may effectively model the nonlinear response of the cochlea if 2D hydrodynamics is considered, using a fitting procedure that determines the parameters of the model by looking for agreement with experimental data. The 2D hydrodynamics can be accounted for either by using the focusing function $\alpha(k)$, or the Green functions formalism.

At the Hopf bifurcation, a dynamical system shows a sharp transition from quiescence to spontaneous self-sustained oscillations, as a function of a parameter ϵ, representing the real part of the system eigenvalues. An oscillating system is represented by two complex conjugate eigenvalues, $\lambda = \epsilon \pm i\omega_r$.

The state with $\epsilon = 0$ is called Hopf bifurcation point and such an oscillator is defined critical. A cubic nonlinearity must operate to stabilize the response.

In ver Hulst (2024) critical oscillators and fluid focusing yield the tall and broad cochlear response through a fitting procedure. A critical oscillator may pump energy into the mechanical system. To see that, we will consider the normal form, which is the linearized system representation in the space of the system eigenvectors of a nonlinear system that can operate at the Hopf bifurcation:

$$\dot{z} = -(\epsilon + i\omega_r)z + (\alpha_H + i\beta_H)z|z|^2 + f. \tag{22}$$

The physical meaning of the terms of this general equation may be different in different models. If the variable z represents the transverse BM displacement, as we will assume in the following discussion, it may be seen as a dynamical equation lacking the inertial term, which turns out to be a good low-frequency approximation in tonotopic systems in which the TW component of frequency ω does not reach the resonant place, and travels therefore in a cochlear region where the local characteristic frequency, associated with the elastic and inertial terms of the oscillator, is larger than ω. Interestingly, this condition is approximately matched, as we have previously noted, by 2D-viscous cochlear models.

If the variable z represents the transverse BM velocity, the equation may be interpreted as a second order equation in the BM displacement, with a nonlinear damping term. ω_r is the characteristic frequency, the parameters α_H (the Lyapunov coefficient) and β_H determine the nonlinear term behavior, and z is a vector with two complex components representing a linear combination of the starting point degrees of freedom. In order to discuss the critical oscillator normal form and its implications we will follow Jülicher et al. (2009).

1.6. Where 2D cochlear models meet Hopf oscillators

In this paper we follow the same idea as ver Hulst (2024), of describing the cochlear dynamics as a coupling between critical oscillators and the fluid, but we will also try to identify the critical oscillators with a realistic physical system, to better understand the role of the active force in this framework. Let we start with a 2DOF schematization of the cochlear micromechanics. For simplicity, the parameters of the two oscillators are considered identical, and equal to those of their internal elastic coupling i.e.: $M_1 = M_2 = M$, $K_1 = K_2 = K_3 = K$, $C_1 = C_2 = C_3 = C$. This may be a rather unrealistic approximation, which is however extremely useful to show the relation between 2DOF low-passed cochlear models and the normal form of Hopf oscillators in the cleanest possible way. In particular, one of the normal modes coincides with the relative motion, on which all the internal forces depend. Relaxing this assumption could be a further step towards a realistic model, which should be taken in further studies, after having highlighted the analytical properties of the solution in the symmetric case. With this assumption, Eq. (10) can be rewritten as:

$$\begin{aligned}
&M\ddot{\xi}_1 + 2C\dot{\xi}_1 + 2\,K\xi_1 = -p_d + C\dot{\xi}_2 + K\xi_2 + p_{OHC}\\
&M\ddot{\xi}_2 + 2C\dot{\xi}_2 + 2\,K\xi_2 = C\dot{\xi}_1 + K\xi_1 - p_{OHC}\\
&\dot{p}_{OHC} + \frac{p_{OHC}}{\tau} = -\frac{K_{nl}}{\tau}(\xi_1 - \xi_2)\\
&\frac{\partial^2 p_d}{\partial x^2} = -2\frac{\rho\alpha}{H}\ddot{\xi}_1.
\end{aligned} \tag{23}$$

A key element of this study is realizing that the two normal modes of the coupled oscillators are the most convenient description of the motion of the system. Indeed, center of mass motion (plus mode) depends (obviously) on the external force only (the differential pressure, as described by a linear equation, while the relative motion (minus mode) is also determined by the nonlinear internal force and may therefore permit a Hopf schematization. If one considers the sum of the first and the second equation, one gets the equation of motion for the center of mass of the system:

$$M(\ddot{\xi}_1 + \ddot{\xi}_2) + C(\dot{\xi}_1 + \dot{\xi}_2) + K(\xi_1 + \xi_2) = -p_d, \tag{24}$$

i.e.:

$$\ddot{X}_+ + \gamma_{cm}(x)\dot{X}_+ + \omega_{0\ cm}^2(x)X_+ = -\frac{p_d}{2M}, \tag{25}$$

where $X_+ = \xi_{cm} = (\xi_1 + \xi_2)/2$, $\gamma_{cm} = C/M$, and $\omega_{0\ cm} = \sqrt{K/M}$ are the local damping coefficient and tonotopic resonance frequency associated with the motion of the center of mass. This equation can be studied separately, as it is independent of the nonlinear OHC force, which, being an internal one, does not affect the motion of the center of mass. Subtracting the second from the first equation, one gets, for the relative motion $X_- = (\xi_1 - \xi_2)/2$ of the two masses:

$$\ddot{X}_- + \gamma(x)\dot{X}_- + \omega_0^2(x)X_- = -\frac{p_d}{2M} + \frac{p_{OHC}}{M}, \tag{26}$$

where $\gamma = 3C/M$ is the total damping of the relative motion, and $\omega_0 = \sqrt{3}\omega_{0\ cm}$ is the characteristic frequency of the relative motion. Note that in the eigenvector space, both normal modes are excited by the differential pressure, while the active force, being an internal one, cannot accelerate the center of mass, and only acts on the equation for the relative motion.

We are now ready to show the connection (and its limitations) between the equation for the normal mode associated to the relative motion forced by an internal active force $F_a = p_{OHC}$ and the normal form of a Hopf oscillator equation described by Jülicher et al. (2009) in a different context. For a forward TW component of frequency $\omega < \omega_0$, i.e. in the path basal to the resonance, where the mass term can be approximately neglected, the oscillatory normal mode for the relative motion is approximately represented by the following system of equations, which we write now in the Jülicher's notation (with the exception of not using $\lambda = m\gamma$ to avoid confusion with the standard name of the eigenvalues) to help the reader understanding the connection:

$$\begin{aligned} m\gamma\dot{X}_- &= -kX_- + F_a + F_{ext} \\ \beta\dot{F}_a &= -F_a - \bar{k}X_-. \end{aligned} \tag{27}$$

where:

- $F_a = p_{OHC}$
- $F_{ext} = p_d$
- $\beta = \tau$
- $m = M$
- $k = 3$ K
- $\bar{k} = K_{nl}$

The second equation describes in this case the low-pass filtering associated with the slow build-up the OHC transmembrane voltage, driven by a current that, in the linear limit, is an elastic function of relative displacement between the two oscillators (Lu et al., 2006). After diagonalization of the system matrix, a single Hopf oscillator equation is obtained in the rotated space for a complex variable z, whose real part coincides with the relative displacement X_-. The details are reported in Appendix. This procedure allows one to write, in the linear approximation, an explicit expression for the admittance of the relative motion mode, as a function of the parameters of the two-oscillator system:

$$Y_- = \frac{\dot{X}_-}{p_d} = \frac{\omega\cos\theta}{\Lambda(\omega - \omega_r - i\epsilon)}, \tag{28}$$

where

$$\epsilon = \frac{1}{2}\left(\frac{k}{m\gamma} + \frac{1}{\beta}\right), \tag{29}$$

$$\omega_r = \sqrt{\frac{\bar{k}}{m\gamma\beta} - \frac{1}{4}\left(\frac{k}{m\gamma} - \frac{1}{\beta}\right)^2}, \tag{30}$$

$$\Lambda = \frac{m\gamma}{\sqrt{1 + \left(\frac{\frac{k}{m\gamma} - \frac{1}{\beta}}{2\omega_r}\right)^2}}, \tag{31}$$

and

$$\theta = \arctan\left(\frac{\frac{k}{m\gamma} - \frac{1}{\beta}}{2\omega_r}\right), \tag{32}$$

In the critical limit $\epsilon \to 0$:

$$Y_- = \frac{\omega\cos\theta}{\Lambda(\omega - \omega_r)}. \tag{33}$$

The admittance of Eq. (33) is real, so it may represent either a damping or an antidamping effect. If $\cos\theta > 0$ and $\omega < \omega_r$, it yields antidamping. As pointed out by ver Hulst (2024), the critical oscillator pumps energy into the system along the TW forward path, before the CF tonotopic region.

Although the striking analogy with the Hopf system described in the literature (Jülicher et al., 2009) may be alluring, the low-frequency assumption is not well verified in the peak region, even considering the basal shift of the response peak due to 2D hydrodynamics (Sisto et al., 2023; Sisto and Moleti, 2024). More importantly, this approximation, which allows one to neglect the second order inertial term in Eq. (26), to exactly match the form of Eq. (27), alters qualitatively the physical meaning of the parameters of the mechanical system. For example, in this two-equation model, the bifurcation cannot be crossed, because ϵ in Eq. (29) is strictly positive, and approaching the critical limit does not even imply optimizing the gain of the system.

1.7. Re-introducing the inertial term in the relative motion equation

It is therefore necessary to take one step forward, to modify and extend the equations for the relative motion by including the mass term. We will show that including the mass term in the equation for the relative motion recovers the expected physical behavior of a Hopf system, in which exceptionally high gain is obtained in the critical region. One gets a system of three first order differential equations:

$$\begin{aligned} \dot{X}_- &= V_- \\ m\dot{V}_- &= -m\gamma V_- - kX_- + F_a + F_{ext} \\ \beta\dot{F}_a &= -F_a - \bar{k}X_-. \end{aligned} \tag{34}$$

The procedure for finding the admittance of the relative motion mode is the same as that described in Appendix. In this case, the 3×3 system matrix is:

$$\mathbf{A3} = \begin{pmatrix} 0 & 1 & 0 \\ B & C & D \\ E & 0 & F \end{pmatrix}, \tag{35}$$

with:

- $B = -\frac{k}{m}$
- $C = -\gamma$
- $D = \frac{1}{m}$
- $E = -\frac{\bar{k}}{\beta}$
- $F = -\frac{1}{\beta}$

The eigenvalue equation is:

$$\lambda^3 + \left(\gamma + \frac{1}{\beta}\right)\lambda^2 + \left(\gamma\beta + \frac{k}{m}\right)\lambda + \frac{\bar{k} + k}{m\beta} = 0. \tag{36}$$

This third order algebraic equation admits one real eigenvalue and, if $\Delta < 0$, the other two eigenvalues are complex conjugates: $\lambda_{1,2} = \epsilon \pm i\omega_r$, with λ_3 real and negative, corresponding therefore to a pure damping mode. Note that we use the same notation as in the appendix for the eigenvalues $\lambda_{1,2}$ and for their real and imaginary parts ϵ and ω_r, although they are relative here to the 3×3 matrix (35), while in the appendix they are eigenvalues of the 2×2 matrix (66), and have a different dependence on the cochlear parameters. The eigenvectors have the form:

$$\vec{v} = \begin{pmatrix} 1 \\ \lambda_i \\ -\frac{E}{F-\lambda_i} \end{pmatrix}, \tag{37}$$

The basis change matrix $\mathbf{P}$ is:

$$\mathbf{P} = \begin{pmatrix} 1 & 1 & 1 \\ \lambda_1 & \lambda_2 & \lambda_3 \\ -\frac{E}{F-\lambda_1} & -\frac{E}{F-\lambda_2} & -\frac{E}{F-\lambda_3} \end{pmatrix}, \tag{38}$$

satisfying the condition:

$$\mathbf{P}^{-1}\mathbf{A}\mathbf{P} = \begin{pmatrix} \lambda_1 & 0 & 0 \\ 0 & \lambda_2 & 0 \\ 0 & 0 & \lambda_3 \end{pmatrix}, \tag{39}$$

If the vector x representing the degrees of freedom in the physical space is real and is given by:

$$\vec{x} = \begin{pmatrix} X_- \\ V_- \\ F_a \end{pmatrix}, \tag{40}$$

The vector y in the rotated space in which $\mathbf{A}$ is diagonal can be written as:

$$\vec{y} = \mathbf{P}^{-1}\vec{x}. \tag{41}$$

The two complex conjugate eigenvalues are associated to complex conjugate components of the vector y:

$$y_1 = y_2^* = z, \tag{42}$$

and, consequently:

$$\vec{y} = \begin{pmatrix} z \\ z^* \\ y_3 \end{pmatrix}, \tag{43}$$

with z complex. In terms of the variables in the rotated space, where $\mathbf{A}$ is diagonal, the system of first order differential equations (34) becomes:

$$\dot{z} = -(\epsilon - i\omega_r)z + f, \tag{44}$$

$$\dot{z}^* = -(\epsilon + i\omega_r)z^* + f^*, \tag{45}$$

$$\dot{y}_3 = \lambda_3 y_3. \tag{46}$$

Only two equations are independent, as the second equation is the complex conjugate of the first. In terms of the complex variable z the system of three equations in the physical space can be set in the form of only two equations. The third one is the time evolution of a purely damped mode ($\lambda_3 < 0$) and does not contribute to the resonant response in the forced case. The first equation represents the normal form of an oscillatory system. As in the previous case, one can interpret it as the linearization of the Hopf oscillator of Eq. (22). The oscillator is at the Hopf bifurcation when $\epsilon = 0$, The forcing term f in the first equation is:

$$f = -\frac{p_d}{m} P_{12}^{-1}. \tag{47}$$

The inverse of the matrix $\mathbf{P}$ can be calculated:

$$\mathbf{P}^{-1} = \frac{1}{det(\mathbf{P})} \begin{pmatrix} \lambda_2 a_3 - \lambda_3 a_2 & a_2 - a_3 & \lambda_3 - \lambda_2 \\ \lambda_3 a_1 - \lambda_1 a_3 & a_3 - a_1 & \lambda_1 - \lambda_3 \\ \lambda_1 a_2 - \lambda_2 a_1 & a_1 - a_2 & \lambda_2 - \lambda_1 \end{pmatrix}, \tag{48}$$

where:

$$a_i = -\frac{E}{F - \lambda_i}, \tag{49}$$

and the determinant is:

$$det(\mathbf{P}) = a_1(\lambda_3 - \lambda_2) + a_2(\lambda_1 - \lambda_3) + a_3(\lambda_2 - \lambda_1). \tag{50}$$

Let us take the equation for z and its complex conjugate and sum up the two:

$$\frac{\partial(z + z^*)}{\partial t} = -\epsilon(z + z^*) + i\omega_r(z - z^*) + f + f^*. \tag{51}$$

The oscillator is at the Hopf bifurcation when $\epsilon = 0$. The displacement of the relative motion can be identified with the real part of the complex coordinate in the rotated space

$$X_- = 2Re(z) = z + z^*. \tag{52}$$

The expression for the velocity can be derived:

$$\dot{X}_- = i\omega(z - z^*) = -2\omega Im(z). \tag{53}$$

Eq. (51) can be rewritten as:

$$\dot{X}_- = -\epsilon X_- + \frac{\omega_r}{\omega}\dot{X}_- + 2Re(f). \tag{54}$$

or:

$$(\omega - \omega_r - i\epsilon)\dot{X}_- = Re(P_{12}^{-1})\omega\frac{p_d}{m}, \tag{55}$$

The admittance can be straightforwardly derived as the ratio between the velocity and the pressure:

$$Y_- = \frac{\dot{X}_-}{p_d} = \frac{Re(P_{12}^{-1})\omega}{m(\omega - \omega_r - i\epsilon)} = \frac{(a_2 - a_3)\omega}{det(\mathbf{P})m(\omega - \omega_r - i\epsilon)}. \tag{56}$$

It is now possible to discuss how the physical parameters of the original model can be set in order to establish specific relations for the parameters of the Hopf oscillator model. It will be useful to define a set of dimensionless quantities:

- $A_{lp} = \frac{1}{\omega_0 \beta}$
- $Q_p = \frac{\omega_0}{\gamma}$
- $r_{OHC} = \sqrt{\frac{\bar{k}}{k}}$
- $CR = \frac{\epsilon}{\omega_r}$

The parameter A_{lp} has a double physical meaning. On one hand, it represents the attenuation factor in the peak region due to low-pass filtering associated with the slow OHC voltage buildup. On the other hand it is associated to the rotation of the phase of the active force, which for large A_{lp} tends to 90°, yielding an effective anti-damping term. In a more realistic model it should be variable along the BM, in this study we consider only one stimulus frequency.

The passive quality factor Q_p is associated with the bandwidth of the BM response at very high stimulus levels (or post-mortem), so it may be assumed of order unity.

The critical ratio (CR) parameter, which measures the distance from the critical limit ($CR \ll 1$), is a function of the other three dimensionless parameters. The expressions for the explicit solutions of third order algebraic equations are rather cumbersome, involving cubic roots. Quite fortunately, the critical condition can also be obtained directly from the eigenvalue Eq. (36), Indeed, the real part of the complex radices of an algebraic equation of the form:

$$x^3 + ax^2 + bx + c = 0 \tag{57}$$

vanishes (critical condition) if $ab = c$, i.e., in this case:

$$\left(\gamma + \frac{1}{\beta}\right)\left(\frac{\gamma}{\beta} + \frac{k}{m}\right) = \frac{\bar{k} + k}{m\beta}. \tag{58}$$

Hence, the dimensionless parameter

$$CR = \left(\frac{\frac{1}{Q^2} + \frac{1}{QA_{lp}} + \frac{A_{lp}}{Q} + 1}{r_{OHC}^2 + 1}\right)^{1/3} - 1 \tag{59}$$

must be much smaller than unity to ensure close-to-critical behavior. If one assumes the passive quality factor Q of order unity, and a constant low-pass attenuation factor A_{lp} of order 10, the critical parameter is approximately given by:

$$CR \approx \left(\frac{1 + 1/Q^2 + A_{lp}/Q}{r_{OHC}^2 + 1}\right)^{1/3} - 1 \tag{60}$$

and the approach to the critical limit is mainly determined, as it should be in a reasonable model, by the dimensionless parameter r_{OHC}, which measures the strength of the nonlinear OHC mechanism. Differently from the 2-equations system of Eq. (27), the bifurcation can be actually crossed for sufficiently strong OHC feedback ($r^2_{OHC} > \frac{1}{Q^2} + \frac{1}{QA_{lp}} + \frac{A_{lp}}{Q}$).

The admittance of the sum mode (the center of mass) is that of a resonant oscillator of frequency $\omega_{0\ cm}$:

$$Y_+ = \frac{\dot{X}_+}{p_d} = \frac{i\omega/m}{\omega^2_{0\ cm} - \omega^2 + i\omega\gamma}. \tag{61}$$

This admittance can also be corrected introducing the viscous friction force on the BM, using the iterative self-consistent procedure described in Sisto et al. (2023). After having found the admittances of the two modes, one can obtain the BM displacement ξ_1, and the RL displacement ξ_2:

$$\dot{\xi}_1 = \frac{Y_+ + Y_-}{2} p_d = Y_1 p_d, \tag{62}$$

$$\dot{\xi}_2 = \frac{Y_+ - Y_-}{2} p_d = Y_2 p_d. \tag{63}$$

2. Results and discussion

We performed simulations in the frequency domain for the linearized system in the WKB approximation for a stimulus frequency of 5 kHz. An iterative procedure was also implemented in order to find self-consistent solutions for the wave vector to account for viscosity. The cochlear model parameters are listed in Table 1, and do not refer to any specific animal. As the model is linear, the different activity levels are parameterized in terms of a globally variable active mechanism efficiency. The results of a first simulation are shown in Fig. 1. The BM gain function shows a large dynamical range, even without getting very close to the critical limit, as shown in Fig. 1. With the parameters of this study, the BM and RL responses are quite similar in amplitude and phase, with a small negative phase shift of the RL response. Another peculiar feature of 2D cochlear models including fluid focusing and viscous drag on the OoC (Sisto et al., 2021), is the progressive basal shift of the response peak (or best place, BP), increasing with decreasing OHC activity (or increasing stimulus level in a nonlinear model). This shift has also experimentally observed in OCT experiments (e.g. Cho and Puria (2022) and Cooper et al. (2018)). Recent 2D models interpret it as a progressive shift of the BP with respect to the "nominal" resonant place, where the considered TW frequency component matches the local $\omega_{0\ cm}$, and which could be called the characteristic place (CP) (Sisto and Moleti, 2024). This feature is also visible in Fig. 1. Another interesting feature of the model simulations is the absence of a sharp admittance peak, i.e., the BM velocity and the pressure responses are similar to each other. This feature is in agreement with experimental results (Dong and Olson, 2013) that showed peaked response across variable stimulus levels for fluid pressure near the BM and estimated similar response for the vertical fluid velocity, which is related to the BM velocity by the adhesion condition. It is also useful to show separately the admittances of the two normal modes (see Fig. 2). The center of mass admittance shows a moderately peaked and level-independent admittance, while the differential motion admittance, which is sensitive to the OHC nonlinear internal force, is a weak function of the activity parameter r_{OHC}. In the Hopf oscillator literature, the study of the system is particularly interesting near the critical point, i.e., where $CR = \epsilon/\omega_r \ll 1$. Fig. 3 shows that approaching the critical limit the gain of the system may become arbitrarily high approaching the critical limit, as a function of the effectiveness of the OHC mechanism, which is a physically expected feature of a critical system. The correspondingly peaked admittance of the relative mode is shown in Fig. 4.

Even in the linear approximation, the sharply peaked response obtained approaching the critical behavior would eventually be smoothed by viscous damping. Introducing increasing viscosity in the simulation with the lowest CR (0.5) of those shown in Fig. 1, the gain is progressively reduced and the peak of the response is further basally shifted, as shown in Fig. 5. Using viscosity coefficients much higher than those of the cochlear fluids may be interpreted as a rough attempt of taking into account the large viscous losses expected inside the viscoelastic elements of the OoC and in the narrow Corti fluid channels within the scala media (Shokrian et al., 2025).

The analysis of the normal form of the linearized equations of a 2DOF cochlear model, including two-dimensional fluid coupling and a low-pass active force, provides a reasonable prediction of the main experimental properties of the BM and RL response, as shown in Fig. 1, without any fine tuning of the cochlear parameters. The normal mode approach allows one to define two separate admittance functions, for the relative motion and the center of mass motion. This formalism

Table 1
Parameters [range] of the cochlear model used in the simulations.

Physical quantity	Name	Value
Stimulus frequency	ω	$2\pi 5000$ rad/s
Tonotopic map scale	k_ω	400 m^{-1}
BM, RL stiffness	$K(x)$	$1.1 * 10^{10} e^{-k_\omega x}$ N/m^3
BM, RL damping	$C(x)$	$10^4 e^{-0.5 k_\omega x}$ N/sm^3
BM, RL mass	M	0.05 kg/m^2
Low-pass attenuation	A_{lp}	10
Passive quality factor	Q	1.35
OHC activity	r_{OHC}	[0.4 – 2.7]
Critical parameter	CR	[1.0 – 0.03]

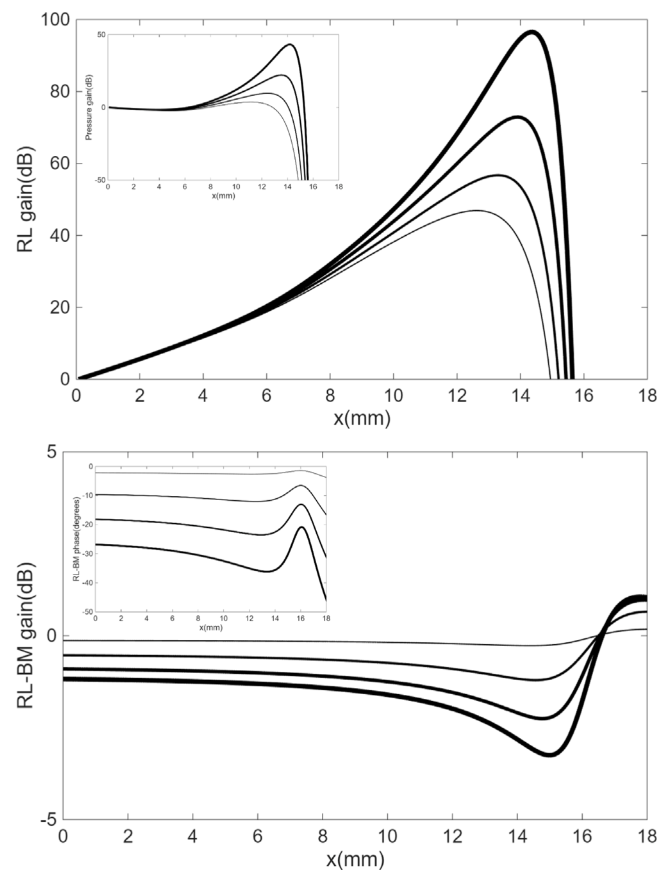

Fig. 1. Top: Simulation of the BM response to a 5 kHz stimulus of a 2DOF 2D cochlear model in the WKB approximation, with parameters chosen in order to simulate the typical range of the BM gain, which increases rapidly with decreasing CR. Lines of increasing thickness are associated to increasing effectiveness of the active mechanism and correspondingly decreasing values of $CR = (1, 0.75, 0.6, 0.5)$. The pressure gain is shown in the inset. Bottom: Difference between the RL and BM gain, and between the RL and BM phase (in the inset)

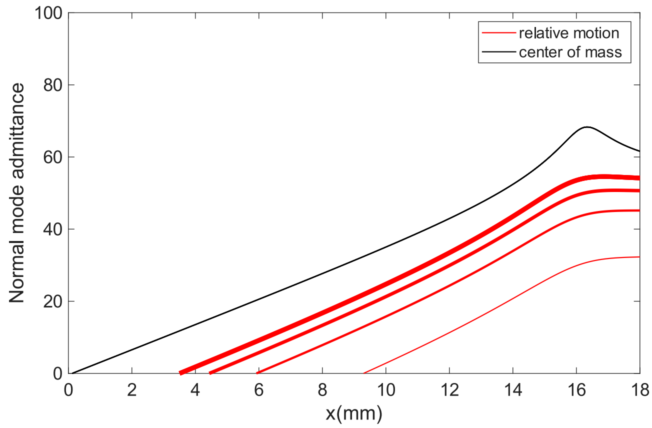

Fig. 2. Admittance of the two modes for the simulations of Fig. 1. The admittance of the relative motion depends on the strength of the active mechanism, i.e., on the critical parameter, but a sufficiently high gain is obtained for the relatively flat admittance corresponding to $CR = 0.5$ (thickest red line).

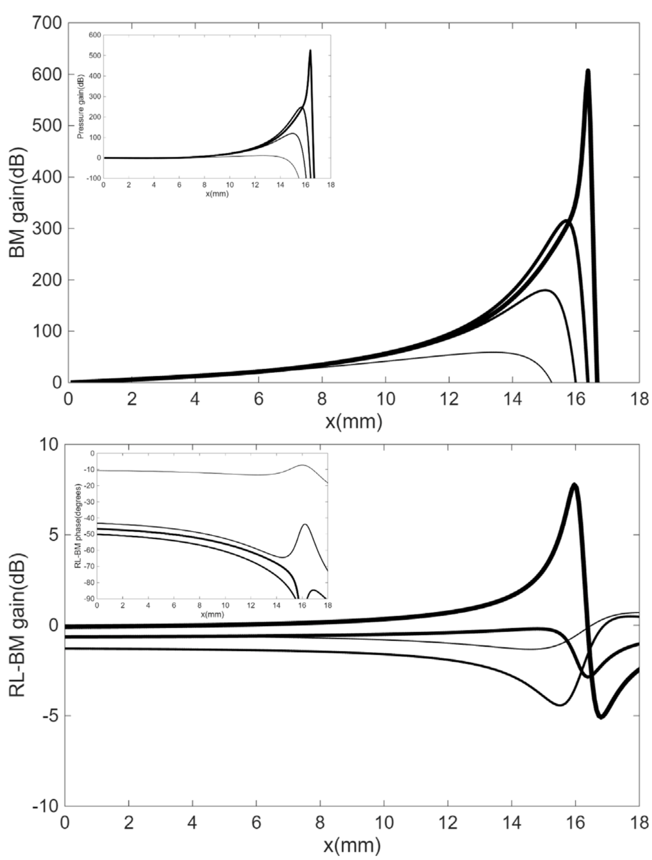

Fig. 3. Top: Simulation of the response to a 5 kHz stimulus of a 2DOF 2D cochlear model in the WKB approximation, using the normal form of the oscillator Eq. (34). The BM and pressure gain functions, defined as the ratio between the local amplitude and that at the cochlear base, are shown as functions of the longitudinal coordinate x, for four different levels of the parameter CR. The four simulations are obtained for $CR = (0.75, 0.3, 0.15, 0.03)$. Approaching the critical limit yields huge gain levels, and very narrow band response. Bottom: Difference between the RL and BM gain, and between the RL and BM phase (in the inset).

provides a direct physical interpretation of the active amplification process and clarifies how the interplay between fluid coupling and

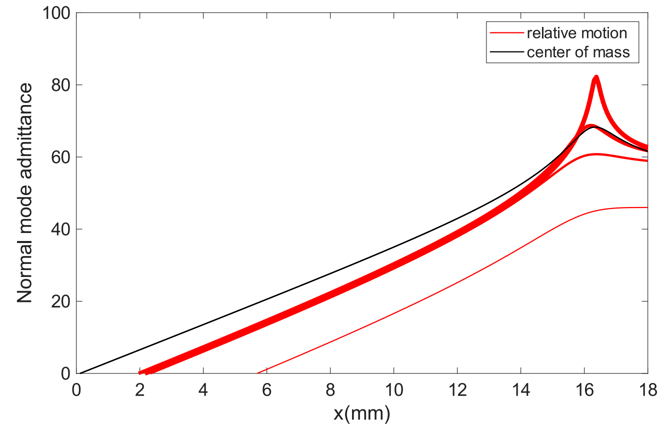

Fig. 4. Admittance of the normal modes for the four simulations of Fig. 3. The admittance of the relative motion mode peaks only for the simulations yielding exceedingly narrow band response and unreasonably high gain.

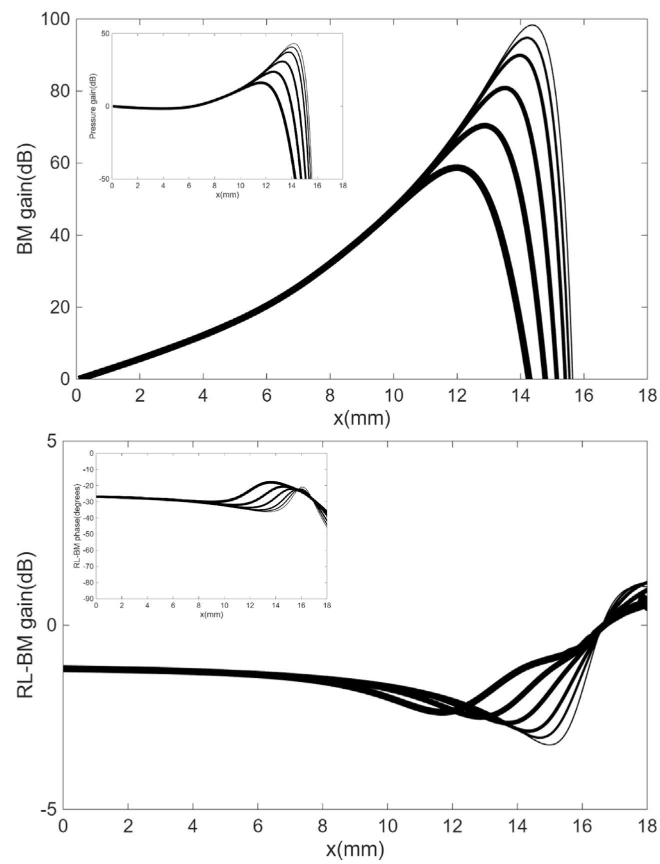

Fig. 5. Top: Simulation of the response to a 5 kHz sinusoidal stimulus of a 2DOF 2D cochlear model in the WKB approximation, as in Fig. 1, for $r_{OHC} = 2.25$, i.e. $CR = 0.5$. Bottom: Difference between the RL and BM gain, and between the RL and BM phase (in the inset). Lines of increasing thickness correspond in this case to increasing values of the viscosity coefficient: $0, \mu_w, 3\mu_w, 10\mu_w, 30\mu_w, 100\mu_w$, where μ_w is the viscosity of water.

active micromechanics gives rise to power gain within the cochlea. Within the present framework, it is shown that the cochlear response increases dramatically as the system approaches the Hopf bifurcation. A key result of this work is that the approach to the critical regime is parameterized entirely in terms of three dimensionless quantities with obvious physical meaning, related to: (1) the effectiveness of the active force generated by the OHCs; (2) the cutoff frequency of the low-pass filter describing the slow build-up of the OHC transmembrane voltage, and (3) the quality factor of the passive mechanical system. This approach provides therefore a transparent and physically grounded interpretation of cochlear criticality: the distance from the Hopf bifurcation is not introduced as an abstract control parameter, but it is naturally associated with measurable physiological properties of the cochlear active process. In this model, it is not necessary to get very close to the critical point to reproduce the experimental cochlear response ($CR = 0.5$ may be a sufficiently small value), which may be considered as a positive feature: fine tuning of the physiological parameters is not necessary to get sufficiently large cochlear gain. As suggested by Fig. 3, exceptionally low values of CR in specific cochlear regions could be one of the conditions (along with geometrical ones Shera, 2007) for getting the particularly strong SOAEs that are sometimes observed, e.g., in newborns (Sisto and Moleti, 1999). Separating the admittance of the relative motion from that of the center of mass is important to get deeper physical insight into the cochlear response. Indeed, the physical properties of the two modes are more clearly identified than those of the two oscillators: the center of mass motion depends on a linear equation driven by the differential pressure only, whereas the relative motion is also determined by the nonlinear active force, as shown in Figs. 2, 4. Finally, in such a scheme, it is possible to introduce viscosity to evaluate its stabilizing effect in the linear limit (see Fig. 5), before introducing the saturating nonlinearity. A realistic compressive response can be ultimately computed only with a numerical time-domain solution of the nonlinear equation system, which is outside the scope of the present paper.

The “identical oscillators” hypothesis is a main limitation of the present study, partially justified by its didactic scope. Indeed, relaxing this hypothesis, which will be necessary to get more accurate predictions of the cochlear response, the analytical properties of the solution that make its physical interpretation so straightforward would not be fully maintained. Another obvious limitation is the use of a linear approximation, which neglects the nonlinear behavior of Hopf oscillators. The aim of this paper was showing the correspondence between two formalisms, which is easily obtained on the linear limit. A detailed analysis of the time-domain response of the locally nonlinear system will be the object of a separate study, dedicated to the prediction of nonlinear effects such as two-tone suppression, intermodulation distortion generation, and self-sustained oscillations.

3. Conclusions

The formalism of critical nonlinear oscillators, which has been the object of several theoretical studies, turns out to be well-tailored to the behavior of 2DOF 2-D cochlear models including a low-passed internal OHC force, pressure focusing and viscous drag. The normal form of the equation of motion, as proposed by Jülicher to describe the dynamics of the hair bundle, turns out to be useful to describe both the relative motion of the BM and RL and the low-pass filtering of the active force with a first order differential equation involving a 2-D variable, while the motion of the center of mass of the OoC is separately described by the usual second order equation driven by the differential pressure only. Analyzing separately these two normal modes enhances physical insight, because only the relative motion mode is sensitive to the internal nonlinear OHC force.

On the other hand, the exact correspondence with the “classical” Jülicher’s form requires neglecting the inertial term in the relative motion mode equation. In this not-well-verified approximation, approaching the critical regime is not always an advantage in terms of peak gain. This unexpected feature suggests that, although formally attractive, the exact correspondence with the Hopf normal form compromises the main physical meaning of the equations. This meaning is fully recovered by restoring the mass term. The generalization of the Jülicher’s formalism to a system of three linear equations, which is presented in this study, leads to a very reasonable relationship between the critical parameter and the three dimensionless parameters associated with the active and passive elements of the system. It is therefore possible to use this approach to tune such a cochlear model with two mechanical degrees of freedom, including 2D hydrodynamic effects, using only three physically meaningful dimensionless parameters.

CRediT authorship contribution statement

Renata Sisto: Writing – original draft, Software, Formal analysis, Conceptualization. **Arturo Moleti:** Writing – review & editing, Writing – original draft, Visualization, Validation, Software, Investigation, Formal analysis, Conceptualization.

Declaration of competing interest

The authors declare that they have no known competing financial interests or personal relationships that could have appeared to influence the work reported in this paper.

Appendix

Here we recall, for the interested reader, the algebraic procedure proposed by Jülicher et al. (2009), to put the two first order differential equations (27) in the normal form, and use it to derive an admittance function for the relative motion mode. Embedding the observable degrees of freedom of the system, X_- and F_a, in a single vector:

$$\vec{Y} = (X_-, F_a), \tag{64}$$

the system can be written in the matrix form::

$$\dot{\vec{Y}} = \mathbf{A}\vec{Y} + \vec{F}_{ext}, \tag{65}$$

where the second component of the vector $\vec{F}_{ext}$ is null.

In the linear limit, by diagonalizing the system matrix:

$$\mathbf{A} = \begin{pmatrix} -\frac{k}{m\gamma} & \frac{1}{m\gamma} \\ -\frac{\bar{k}}{\beta} & -\frac{1}{\beta} \end{pmatrix}, \tag{66}$$

one gets the system eigenvalues λ_1 and λ_2, which are complex conjugates, implying a resonant damped oscillatory solution for the homogeneous system:

$$\lambda_{1,2} = -(\epsilon \pm i\omega_r), \tag{67}$$

With damping ϵ and resonance frequency ω_r given, respectively, by:

$$\epsilon = \frac{1}{2}\left(\frac{k}{m\gamma} + \frac{1}{\beta}\right), \tag{68}$$

$$\omega_r = \sqrt{\frac{\bar{k}}{m\gamma\beta} - \frac{1}{4}\left(\frac{k}{m\gamma} - \frac{1}{\beta}\right)^2}. \tag{69}$$

The basis change matrix $\mathbf{V}$ can be written in terms of the eigenvector u:

$$u = m\gamma\left[i\omega_r + \frac{1}{2}\left(\frac{k}{m\gamma} - \frac{1}{\beta}\right)\right], \tag{70}$$

and its complex conjugate u^*, as:

$$\mathbf{V}^{-1} = \frac{2}{u - u^*}\begin{pmatrix} u & -1 \\ -u^* & 1 \end{pmatrix}, \tag{71}$$

The complex variable z is one of the components of a complex vector $\vec{z}$ that can be written in the rotated space in which $\mathbf{A}$ is diagonal:

$$\vec{z} = \mathbf{V}^{-1}\vec{Y}. \tag{72}$$

The two components of z are complex conjugate, so the non-homogeneous system can be written as a single equation

$$\dot{z} = -(\epsilon - i\omega_r)z + f, \tag{73}$$

where

$$f_1 = f = V_{11}^{-1}\frac{p_d}{m\gamma} = \frac{2u}{u-u^*}\frac{p_d}{m\gamma} = \frac{i\omega_r\left[1+\frac{1}{2i\omega_r}\left(\frac{k}{m\gamma}-\frac{1}{\beta}\right)\right]}{i\omega_r}\frac{p_d}{m\gamma} = \left[1-\frac{i}{2\omega_r}\left(\frac{k}{m\gamma}-\frac{1}{\beta}\right)\right]\frac{p_d}{m\gamma} = p_d\frac{e^{i\theta}}{\Lambda}. \tag{74}$$

The pressure (assumed real for simplicity) in the rotated space yields a complex stimulus of amplitude (Jülicher et al., 2009):

$$\frac{p_d}{\Lambda} = \frac{p_d\sqrt{1+\left(\frac{\frac{k}{m\gamma}-\frac{1}{\beta}}{2\omega_r}\right)^2}}{m\gamma}, \tag{75}$$

and phase:

$$\theta = \arctan\left(\frac{\frac{k}{m\gamma}-\frac{1}{\beta}}{2\omega_r}\right), \tag{76}$$

Eq. (73) can be considered as the linearized normal form of the dynamical equation of a nonlinear oscillator:

$$\dot{z} = -(\epsilon - i\omega_r)z + (\alpha_{nl} + i\beta_{nl})z|z|^2 + f. \tag{77}$$

The relative displacement between the two masses of the OoC can be identified with the real part of the complex coordinate z:

$$X_- = Re(z) = \frac{z+z^*}{2}. \tag{78}$$

It can be straightforwardly demonstrated that $Im(z)$ can be written as:

$$Im(z) = \frac{1}{m\gamma\omega_r} - \left[F_a + X_-\frac{m\gamma}{4}\left(\frac{k}{m\gamma}-\frac{1}{\beta}\right)\right]. \tag{79}$$

Let us take the complex conjugate of the linearized Eq. (73) and sum them up:

$$(\dot{z}+\dot{z}^*) = -\epsilon(z+z^*) + i\omega_r(z-z^*) + f + f^*, \tag{80}$$

The velocity can be derived in the frequency domain as:

$$\dot{X}_- = i\omega\frac{z-z^*}{2} = -\omega Im(z), \tag{81}$$

hence:

$$(\omega-\omega_r)\dot{X}_- = -\epsilon\omega X_- + \omega Re(f). \tag{82}$$

or:

$$(\omega-\omega_r-i\epsilon)\dot{X}_- = \omega\frac{\cos\theta}{\Lambda}p_d, \tag{83}$$

The admittance of the relative motion mode can be straightforwardly derived as the ratio between the velocity and the pressure:

$$Y_- = \frac{\dot{X}_-}{p_d} = \frac{\omega\cos\theta}{\Lambda(\omega-\omega_r-i\epsilon)}. \tag{84}$$

References

Allen, J., 1977. Two-dimensional cochlear fluid model: New results. J. Acoust. Soc. Am. 61, 110–119.

Allen, J., Sondhi, M., 1979. Cochlear macromechanics: Time domain solutions. J. Acoust. Soc. Am. 66, 123–132.

Altoè, A., Shera, C., 2020. The cochlear ear horn: Geometric origin of tonotopic variations in auditory signal processing. Sci. Rep. 10, 20528.

Altoè, A., Shera, C., 2023. The long outer-hair-cell RC time constant: A feature, not a bug, of the mammalian cochlea. J. Assoc. Res. Otolaryngol. 24, 129–145.

Berger, J., Rubinstein, J., 2021. A flexible anatomical set of mechanical models for the organ of corti. R. Soc. Open Sci. 8 (9), 210016.

Cartwright, J.H.E., González, D.L., Piro, O., 1999. Nonlinear dynamics of the perceived pitch of complex sounds. Phys. Rev. Lett. 82, 5389–5392.

Cho, N.H., Puria, S., 2022. Cochlear motion across the reticular lamina implies that it is not a stiff plate. Sci. Rep. 12, 18715.

Cooper, N.P., Vavakou, A., van der Heijden, M., 2018. Vibration hotspots reveal longitudinal funneling of sound-evoked motion in the mammalian cochlea. Nat. Commun. 3, 3054.

Dong, W., Olson, E.S., 2013. Detection of cochlear amplification and its activation. Biophys. J. 105, 1067–1078.

Duifhuis, H., 2012. Cochlear Mechanics: Introduction to a Time Domain Analysis of the Nonlinear Cochlea. Springer, Berlin/Heidelberg.

Eguíluz, V.M., Ospeck, M., Choe, Y., Hudspeth, A.J., Magnasco, M.O., 2000. Essential nonlinearities in hearing. Phys. Rev. Lett. 84, 5232–5235.

Iwasa, K.H., Adachi, M., 1997. Force generation in the outer hair cell of the cochlea. Biophys. J. 73, 546–555.

Jülicher, F., Dierkes, K., Lindner, B., et al., 2009. Spontaneous movements and linear response of a noisy oscillator. Eur. Phys. J. E 29, 449–460.

Lee, H.Y., Raphael, P.D., Xia, A., Kim, J., Grillet, N., Applegate, B.E., Ellerbee Bowden, A.K., Oghalai, J.S., 2016. Two-dimensional cochlear micromechanics measured in vivo demonstrate radial tuning within the mouse organ of corti. J. Neurosci. 36 (31), 8160–8173.

Lu, T.K., Zhak, S., Dallos, P., Sarpeshkar, R., 2006. Fast cochlear amplification with slow outer hair cells. Hear. Res. 214, 45–67.

Moleti, A., Sisto, R., 2025. Optimizing the diagnostic power of otoacoustic emissions using theoretical cochlear mechanics. In: Mathematical Models of the Cochlear Function (Chapter 3). Springer, Switzerland, pp. 27–80.

Neely, S.T., Kim, D.O., 1986. A model for active elements in cochlear biomechanics. J. Acoust. Soc. Am. 79, 1472–1480.

Shera, C.A., 2007. Laser amplification with a twist: Traveling-wave propagation and gain functions from throughout the cochlea. J. Acoust. Soc. Am. 122, 2738–2758.

Shera, C.A., Tubis, A., Talmadge, C.L., 2005. Coherent reflection in a two-dimensional cochlea: Short-wave versus long-wave scattering in the generation of reflection-source otoacoustic emissions. J. Acoust. Soc. Am. 118, 287–313.

Shokrian, M., Lin, W.-C., Macić, A., Nam, J.-H., 2025. Corti fluid is a medium for outer hair cell force transmission. J. Neurosci. 45.

Sisto, R., Belardinelli, D., Altoè, A., Shera, C.A., Moleti, A., 2023. Crucial 3-D viscous hydrodynamic contributions to the theoretical modeling of the cochlear response. J. Acoust. Soc. Am. 153, 77–86.

Sisto, R., Belardinelli, D., Moleti, A., 2021. Fluid focusing and viscosity allow high gain and stability of the cochlear response. J. Acoust. Soc. Am. 150, 4283.

Sisto, R., Moleti, A., 1999. Modeling otoacoustic emission by active nonlinear oscillators. J. Acoust. Soc. Am. 106, 1893–1906.

Sisto, R., Moleti, A., 2021. Low-passed outer hair cell response and apical-basal transition in a nonlinear transmission-line cochlear model. J. Acoust. Soc. Am. 149, 1296–1305.

Sisto, R., Moleti, A., 2024. The tonotopic cochlea puzzle: A resonant transmission line with a “non-resonant” response peak. JASA Express Lett. 4, 074401.

Sisto, R., Moleti, A., 2025. Contribution of the reticular lamina motion to the traveling wave: a WKB approach. Hear. Res. 464, 109324.

Sisto, R., Moleti, A., Altoè, A., 2015. Decoupling the level dependence of the basilar membrane gain and phase in nonlinear cochlea models. J. Acoust. Soc. Am. 138, EL155–EL160.

Sisto, R., Shera, C.A., Altoè, A., Moleti, A., 2019. Constraints imposed by zero-crossing invariance on cochlear models with two mechanical degrees of freedom. J. Acoust. Soc. Am. 146, 1685–1695.

Steele, C.R., Taber, L.A., 1979. Comparison of WKB calculations and experimental results for three-dimensional cochlear models. J. Acoust. Soc. Am. 65, 1007–1018.

ver Hulst, H., 2024. Marrying the Physics of Critical Oscillators with Traveling-Wave Models of the Cochlea (Ph.D. thesis). Université PSL Paris.